TABLE I. Comparison of the experimental $E2$ transition probabilities with the theoretical estimates.

Nucleus	$I_i \rightarrow I_f$	Energy (keV)	$T_{1/2}$	$B(E2)/(2I_f+1)$ in units of 10^{-50} $e^2\times$cm^4 experimental	Sorensen estimate	Single-particle estimate
Pr^{141}	$\frac{7}{2} \rightarrow \frac{5}{2}$	145.44	(1.91±0.06) nsec	0.021±0.016	0.0008	0.010
Te^{123}	$\frac{3}{2} \rightarrow \frac{1}{2}$	159.0	(19.85±1.0)×10^{-11} sec	1.29±0.95	0.86	0.180
Hg^{199}	$\frac{5}{2} \rightarrow \frac{1}{2}$	158.4	(2.37±0.07) nsec	6.25±1.26	2.64	0.350
Hg^{199}	$\frac{3}{2} \rightarrow \frac{1}{2}$	208.2	(7.13±0.7)×10^{-11} sec	5.28±0.75	0.44	0.350
Ir^{191}	$\frac{5}{2} \rightarrow \frac{3}{2}$	129.4	(12.53±1.25)×10^{-11} sec	23.6±2.7	7.35	0.047

the following relation:

$$T(E2)=1.225\times10^{61}E_\gamma{}^5B(E2),$$

where E_γ is the energy in MeV and $B(E2)$ in units of $e^2\times$cm^4. The energy values used[15,18] here are 145.44 and 159.00 keV. These experimental reduced transition probabilities are shown in Table I as $B(E2)/(2I_f+1)$, where I_f is the final angular momentum, together with the theoretical calculation made by Sorensen[2] and single-particle estimates. In the same table, the work on the nuclei Hg^{190} and Ir^{191} (Refs. 4 and 5) are also included. The experimental $B(E2)$ values in Table I are given with errors arising from the uncertainties in the measured lifetime, and the assumed values of internal conversion, admixture, and branching ratios.

[18] W. W. Black and R. L. Heath, Nucl. Phys. **A90**, 650 (1967).

PHYSICAL REVIEW VOLUME 165, NUMBER 4 20 JANUARY 1968

$In^{113}(n,\gamma)In^{114m,114g}$, $In^{113}(n,n')In^{113m}$, $In^{115}(n,\gamma)In^{116m,116g}$, and $In^{115}(n,n')In^{115m}$ Activation Cross Sections between 0.36 and 1.02 MeV*

H. A. GRENCH AND H. O. MENLOVE†
Lockheed Palo Alto Research Laboratory, Palo Alto, California
(Received 28 August 1967)

The $In^{113}(n,\gamma)In^{114m,114g}$, $In^{113}(n,n')In^{113m}$, $In^{115}(n,\gamma)In^{116m,116g}$, and $In^{115}(n,n')In^{115m}$ activation cross sections have been measured at 11 neutron energies between approximately 0.36 and 1.02 MeV. The full neutron energy spread was, on the average, about 0.06 MeV for the irradiations. All cross sections were measured relative to the $Au^{197}(n,\gamma)Au^{198}$ activation cross section. Normalizations of the relative cross sections for formation of In^{114g}(72 sec) and of In^{116g}(14 sec) were obtained from the results of thermal-neutron irradiations by using the reported thermal-cross-section values. Efficiency calibration of a NaI(Tl) crystal made it possible to obtain the magnitudes of the cross section for the other four reactions. Comparisons of the experimental results with calculations based on the statistical theory of nuclear reactions have been made.

INTRODUCTION

THE statistical model of nuclear reactions has been widely used, but with varying degrees of success, in making predictions of energy-averaged cross sections as well as in calculating individual and average properties of nuclear energy levels. The present work on three fast-neutron activation cross sections (capture leading to metastable and ground states, and inelastic scattering) for each of the two stable In isotopes was carried out primarily in order to see with what accuracy the statistical model could predict all of the cross sections with a self-consistent set of parameters. This set would be fixed as much as possible from the results of other types of experiments. Additionally, it was hoped that information on the spin of the second excited state of In^{113} could be obtained from comparison of the measured and calculated $In^{113}(n,n')In^{113m}$ cross sections.

Accurate calculations and measurements of fast-neutron inelastic-scattering and capture cross sections have great practical significance, particularly in relation to the energy and flux degradation processes occurring in nuclear reactors. There is also considerable specific interest in the $In^{115}(n,n')In^{115m}$ cross section, since determinations of the shape and intensity of reactor-neutron spectra via the threshold-detector technique[1] have often made use of this reaction.

Table I lists the In activation cross sections which

* This work was supported by the Lockheed Independent Research Program and the U. S. Atomic Energy Commission.
† Present address: Los Alamos Scientific Laboratory, University of California, Los Alamos, N. M.

[1] W. N. McElroy, R. C. Barrall, and D. Ewing, Air Force Weapons Laboratory Technical Report No. AFWL-TR-65-34, 1965, Vol. 1 (unpublished).

were measured between neutron energies of approximately 0.36 and 1.02 MeV. The half-lives which are listed in Table I are weighted averages of the values given in Ref. 2 that have errors quoted, and the half-life uncertainties tabulated were obtained using the quoted errors. An exception to this occurs for In^{114g} (72 sec) where no half-life uncertainty is given in Ref. 2.

The cross sections leading to the four longest-lived activities were obtained by counting predominant decay γ rays. Since the cross sections reported here were obtained relative to the $Au^{197}(n,\gamma)Au^{198}$ activation cross section, γ-ray counting efficiencies relative to that for the Au^{198} 412-keV γ ray were needed. For the two shortest-lived activities for which the number of γ rays per decay is small and β rays had to be counted, normalizations of the cross sections were obtained from the results of thermal irradiations, using published thermal-activation-cross-section values. Preliminary descriptions of the present experimental results and their interpretation have been presented previously.[3-6] The results in the present paper supersede those reported earlier as preliminary results.[3-7]

DECAY CHARACTERISTICS

Some of the decay-scheme features pertinent to calculations of cross sections from the experimental data as well as to theoretical interpretations of the results are shown in Figs. 1 and 2. The information given in these figures was obtained from a review of the literature. A summary of particularly pertinent aspects of the decay schemes will be given here.

The spin and parity assignments shown in Fig. 1 for the ground and first excited states of In^{113} are well established.[2] The second excited state[2] occurs at 0.648 MeV. This level was assigned spin and parity $\frac{1}{2}^-$ or $\frac{3}{2}^-$ on the basis of work[8] which indicated that the 255-keV transition was most probably of $M1$ or $(M1+E2)$ character. Other experiments[9] which indicated a weak crossover transition led to a $\frac{5}{2}^-$ assignment. One of the purposes of the present experiment was to try to resolve this discrepancy by an independent method, namely, by comparing experimental values with the results of theoretical calculations for the $In^{113}(n,n')In^{113m}$ activation cross section in the energy region just above the excitation threshold of the 648-keV level. The next known level[10] of In^{113} is at 1.026 MeV.

TABLE I. The measured activation cross sections and the half-lives adopted for data analysis.

Reaction	Half-life of product nucleus
$In^{113}(n,\gamma)\ In^{114m}$	50.0 ±0.2 day
$In^{113}(n,\gamma)\ In^{114g}$	72 sec
$In^{113}(n,n')In^{113m}$	1.72±0.02 h
$In^{115}(n,\gamma)\ In^{116m}$	54.13±0.04 min
$In^{115}(n,\gamma)\ In^{116g}$	14.0 ±0.3 sec
$In^{115}(n,n')In^{115m}$	4.50±0.02 h

The 393-keV γ ray was counted to obtain the $In^{113}(n,n')In^{113m}$ reaction yield. The number of these γ rays per In^{113m} decay, therefore, had to be known. Measurements of the total-internal-conversion coefficient for the 393-keV transition reported in Ref. 2 exhibit disagreements which cannot be accounted for on the basis of the quoted uncertainties of the results. Therefore, the result of a more recent measurement[11] of higher quoted precision has been used in the present cross-section calculations. This result is $\alpha=0.528\pm0.009$, which gives a value of 0.654 ± 0.011 393-keV γ rays per In^{113m} decay.

The 192-keV γ ray of In^{114m} was counted in order to obtain the $In^{113}(n,\gamma)In^{114m}$ reaction yield. The total-internal-conversion coefficient for this transition, 4.4 ± 0.4, was obtained by finding the weighted average of the two most precise measurements quoted in Ref. 2. These two measurements are in good agreement. The value 3.5% was adopted for the percentage of decays of this state by electron capture. No error was quoted in

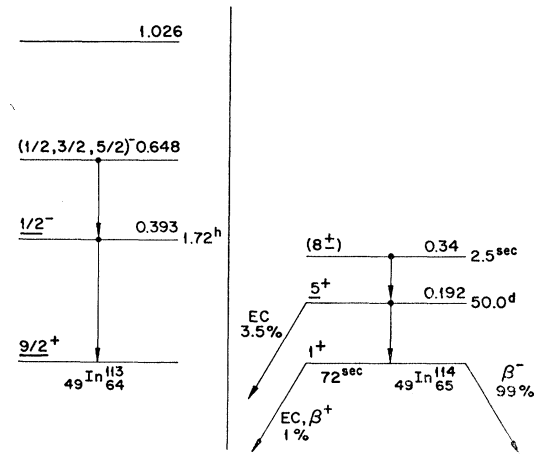

FIG. 1. Decay schemes of low-lying levels of In^{113} and In^{114}.

[2] *Nuclear Data Sheets*, compiled by K. Way *et al.* (Printing and Publishing Office, National Academy of Sciences—National Research Council, Washington, D. C., 1960).
[3] H. A. Grench and H. O. Menlove, Bull. Am. Phys. Soc. **8**, 478 (1963).
[4] H. A. Grench and H. O. Menlove, Bull. Am. Phys. Soc. **9**, 21 (1964).
[5] H. A. Grench, in *Nuclear Spin-Parity Assignments*, edited by N. B. Gove and R. L. Robinson (Academic Press Inc., New York, 1966), p. 297; Bull. Am. Phys. Soc. **11**, 597 (1966).
[6] H. A. Grench, U. S. Atomic Energy Commission Report No. CONF-660303, Book 2, p. 742 (unpublished); Bull. Am. Phys. Soc. **11**, 655 (1966).
[7] *Brookhaven National Laboratory Report No. BNL-325* (U.S. Government Printing Office, Washington, D.C., 1966), 2nd ed., Suppl. 2, Vol IIB.
[8] S. B. Burson, H. A. Grench, and L. C. Schmid, Phys. Rev. **115**, 188 (1959).
[9] W. E. Phillips and J. I. Hopkins, Phys. Rev. **119**, 1315 (1960).
[10] E. M. Bernstein, G. G. Seaman, and J. M. Palms, Bull. Am. Phys. Soc. **12**, 19 (1967).
[11] S. K. Sen and I. O. Durosinmi-Etti, Phys. Letters **18**, 144 (1965).

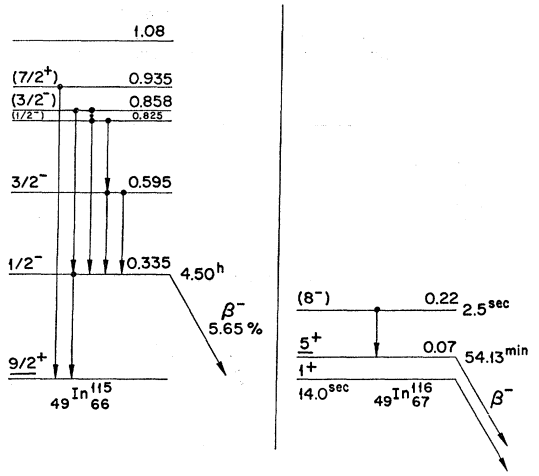

FIG. 2. Decay schemes of low-lying levels of In^{115} and In^{116}.

the literature for this percentage. The number of 192-keV γ rays per In^{114m} decay is therefore 0.179 $\pm$0.013, where it is assumed that the error introduced by the uncertainty in the amount of electron capture is negligible compared to that from the uncertainty in the internal-conversion coefficient. The 72-sec ground state decays by β emission about 99% of the time[2] to the ground state of Sn^{114}. The spin-parity assignments of both the 50-day and 72-sec states are well established.[2]

The In^{115} level scheme is shown in Fig. 2. The spin-parity assignments of the ground and first excited states of In^{115} are unambiguous.[2] Recent measurements[12] by directional-correlation techniques have shown that the 595-keV state has a $\frac{3}{2}^-$ character. The spin-parity assignments for the higher-lying states are still quite uncertain.[2,12]

The In^{115m} yield was determined by counting the 335-keV γ ray. A weighted average of the two most recent measurements[13,14] of the total-internal-conversion coefficient of this transition yields $\alpha=0.89\pm0.05$. β decay from this state occurs 5.65% of the time.[15,16] Combination of these quantities, assuming no error is contributed by the uncertainty in the β-decay percentage, gives 0.499$\pm$0.013 335-keV γ rays per In^{115m} decay. This agrees well with the result obtained by Heertje *et al.*,[17] who also reviewed the literature and arrived at the value 0.50$\pm$0.02.

The yield of the $In^{115}(n,\gamma)In^{116m}$ reaction was obtained by counting the 1.27-MeV γ ray emitted from Sn^{116} following the 54-min decay. A weighted average of results recently summarized by Bolotin[18] yields 0.82$\pm$0.03 1.27-MeV γ rays per 54-min decay. The 14-sec ground state of In^{116} decays by β emission over 98% of the time[19] to the ground state of Sn^{116}. The spin-parity assignment of the 54-min state has been established.[2] Although the assignment for the ground state no longer[18,19] seems ambiguous, that of the 2.5-sec state is in great doubt.[20]

Finally, the value used for the number of 0.412-MeV γ rays per Au^{198} decay[21] was 0.960$\pm$0.005.

EXPERIMENTS AND RESULTS

Introduction

The experimental arrangement was similar to that described previously.[21] Fast neutrons were produced via the $Li^7(p,n)Be^7$ reaction. Irradiations were performed at 11 neutron energies between 0.36 and 1.02 MeV using Li targets which were on the average about 37-keV thick at the source-reaction threshold. The lithium was vacuum-evaporated onto a 0.005-in.-thick Ta backing. The In cross sections were determined as a function of energy relative to the $Au^{197}(n,\gamma)Au^{198}$ activation cross section. Samples of high-purity natural In_2O_3 (4.28% In^{113} and 95.72% In^{115}; denoted here as $In^{115}{}_2O_3$) and of $In^{113}{}_2O_3$ (94.51% In^{113} and 5.49% In^{115}) were contained in cylindrical Plexiglas capsules, each of which had 0.015-in.-thick faces, a 0.060-in. wall thickness, and a 0.688-in. inside diameter. The oxide samples (3 of $In^{115}{}_2O_3$ and 2 of $In^{113}{}_2O_3$) ranged in weight from 0.173 to 0.177 g. Circular Au foils, 0.005 in. thick, were activated along with the In_2O_3 samples. The In_2O_3 samples were sandwiched between Au foils. This packet was mounted about 1 in. from the Ta backing and at 0° to the proton beam line. The neutron flux was monitored by means of a "long counter" placed about 3 m away and at 0° to the beam axis, so that any time variation of the flux could be taken into account in the cross-section calculations. The experimental techniques employed for the production of the four longest-lived activities differed somewhat from those used when the two shortest-lived activities were produced; hence, the discussion of experimental procedures will be divided into two parts.

Long-Lived Activities

Experiments

The irradiation geometry used in the determination of the $In^{113}(n,n')In^{113m}$, $In^{113}(n,\gamma)In^{114m}$, $In^{115}(n,n')In^{115m}$, and $In^{115}(n,\gamma)In^{116m}$ activation cross sections is shown

[12] V. R. Pandharipande, K. G. Prasad, R. M. Singru, and R. P. Sharma, Phys. Rev. **143**, 740 (1966).
[13] I. A. Antonova and I. V. Estulin, Izv. Akad. Nauk SSSR, Ser. Fiz. **18**, 79 (1954).
[14] I. V. Estulin and E. M. Moiseeva, Zh. Eksperim. i Teor. Fiz. **28**, 541 (1955) [English transl.: Soviet Phys.—JETP **1**, 463 (1955)].
[15] P. R. Bell, B. H. Ketelle, and J. M. Cassidy, Phys. Rev. **76**, 574 (1949).
[16] L. M. Langer, R. D. Moffat, and G. A. Graves, Phys. Rev. **86**, 632A (1952).
[17] I. Heertje, W. Nagel, and A. H. W. Aten, Jr., Physica **30**, 775 (1964).
[18] H. H. Bolotin, Phys. Rev. **136**, B1557 (1964).
[19] P. Fettweiss and J. Vervier, Phys. Letters **3**, 36 (1962).
[20] W. Pönitz, Nucl. Phys. **66**, 297 (1966).
[21] H. A. Grench, Phys. Rev. **140**, B1277 (1965).

schematically in Fig. 3. Three gold foils were employed in each irradiation, as shown in the figure, so that the average neutron flux at the position of each In_2O_3 sample could be found.

After irradiation, the two In_2O_3 samples were counted alternately on a 4-in.-diam×4-in. NaI(Tl) crystal. Each sample was placed on the face of the crystal housing and coaxially with the crystal. Spectra were usually recorded in a 100-channel pulse-height analyzer. Several spectra from each sample were accumulated over a time interval long enough that the relative amounts of 54-min, 1.7-h, 4.5-h, and 50-day activities changed considerably.

The similarity of the $In^{113}{}_2O_3$ and the $In^{115}{}_2O_3$ samples and the fact that they were counted on the same crystal were useful in connection with the data analysis. Figure 4, showing the spectra (corrected for room background) obtained for $In^{113}{}_2O_3$ and for $In^{115}{}_2O_3$, will be used to illustrate the separation of the various activities. The $In^{115}{}_2O_3$ spectrum shown in the figure was obtained in a 1-h count which started 51 min after the end of a 280-min irradiation by neutrons with an average energy of 0.834 MeV; the $In^{113}{}_2O_3$ spectrum shown was obtained in a 1-h count which started 121 min after the end of the irradiation. It was found that the 50-day activity was negligible in the $In^{115}{}_2O_3$ sample. A spectrum obtained after the other activities had decayed away was used to subtract out the counts, channel-by-channel, for the 50-day activity in the $In^{113}{}_2O_3$ spectrum. After this was done, the total counts for each sample included in the region of the 1.09- and 1.27-MeV peaks of In^{116m} were used to obtain the normalization factor necessary to subtract the In^{116m} (obtained from the $In^{115}{}_2O_3$ sample) from the $In^{113}{}_2O_3$ spectrum. The result was a "pure" In^{113m} spectrum; a Gaussian fit was made to obtain the area under the 393-keV peak. The 335-keV γ ray from In^{115m} had not been quite properly subtracted out in this process, but the error involved was found to be negligible. One or more later counts of the $In^{115}{}_2O_3$ sample were used to obtain the 4.5-h activity. In this case, the region under the 1.09- and 1.27-MeV peaks was again used for normalization to subtract out the 54-min counts obtained from the early run shown. A correction was made to account for

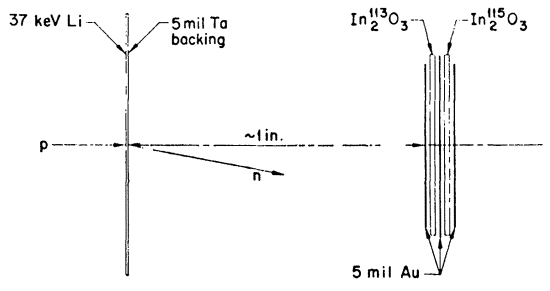

FIG. 3. Schematic diagram of irradiation geometry for production of long-lived activities.

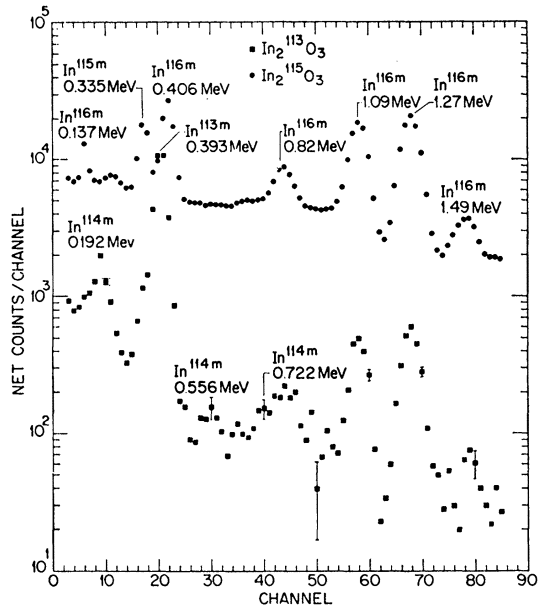

FIG. 4. Gamma-ray spectra of $In^{113}{}_2O_3$ and $In^{115}{}_2O_3$ samples recorded under conditions described in the text. Predominant γ rays are identified. Room background has been subtracted.

the 4.5-h activity subtracted in this process. A Gaussian fit to the 335-keV peak in In^{115m} was used to obtain the 4.5-h yield. This rather complicated procedure was judged to be more accurate than an ordinary decomposition of total counts in a region of the spectrum into half-life components. The In^{116m} counts were obtained from the area under the 0.61- to 1.42-MeV region of the spectrum from the $In^{115}{}_2O_3$ sample.

The $In^{113}{}_2O_3$ sample was also counted on a 2-in.-diam ×0.25-in. NaI(Tl) crystal after other activities had decayed away in order to obtain the 50-day component. The counts in the channels encompassing the region of the 192-keV peak were used to obtain the yield of this activity.

The Au foils were counted individually on the 4-in.-diam×4-in. crystal in the same geometry as the In_2O_3 samples. The area under a Gaussian curve fit to the 412-keV γ-ray peak was used to obtain the Au^{198} activity.

The 4-in.×4-in. NaI(Tl) crystal had been previously calibrated[21,22] for point sources on the crystal axis, at both 0 in. and 6 in. from the face of the crystal housing. Since the 50-day yield had been determined from counting on the 2-in.×0.25-in. crystal, supplementary experiments were performed in which the 50-day activity of an $In^{113}{}_2O_3$ source was counted on both crystals. The area under a Gaussian curve fit to the data from the larger crystal for the 192-keV peak was used to normalize the data obtained from the smaller crystal.

Supplementary experiments were performed for the determination of corrections due to small effects such

[22] J. H. Rowland (private communication).

as γ-ray self-absorption in the In_2O_3 and holder, and finite dimensions of the sources. The area under the region of the 54-min spectrum between 0.61 and 1.42 MeV also had to be related to the area under a Gaussian fit to the 1.27-MeV peak. This was done by counting an $In^{115}{}_2O_3$ sample for the 54-min activity in the usual geometry and at 6 in. from the face of the crystal housing. This larger distance was necessary because of the large γ-ray summing effects observed when the sample was counted directly on the crystal housing. A point source of Zn^{65} (1.17 MeV) was used to check the 0 in. to 6 in. peak-area ratio. The remaining small summing effects at 6 in. for the 1.27-MeV γ ray of In^{116m} were also determined and taken into account.

Since the final value for the amount of 50-day activity produced depended upon the large internal-conversion coefficient for the 192-keV transition, which was known to only $\pm 10\%$ accuracy, a separate experiment was performed to check this method of obtaining the 50-day yield. A point source of In^{114m} was made by depositing a solution[23] of $In^{114m}Cl$ in HCl on a thin film. This was counted in a 4π split proportional counter, using coincidence-anticoincidence techniques[24] between halves of the chamber, in order to obtain the absolute disintegration rate of the source. The source was then enclosed in In_2O_3 in its capsule and counted on the small NaI(Tl) crystal in the usual way. In this manner the counts in the 192-keV region of the spectrum could be directly related to the 50-day disintegration rate. The over-all counting efficiency obtained in this way was in good agreement with that obtained using the calibration of the 4-in.$\times$4-in. crystal and the internal-conversion coefficient. An average of the results employing the two methods was used in final cross-section calculations.

Supplementary experiments were performed in order to determine the effect of scattered neutrons on cross-section determinations. Two successive irradiations in different geometries were performed at each of three energies. One geometrical arrangement was that of a usual irradiation except that a 0.030-in.-thick In-metal disk and an additional Au foil were placed in the center of the packet. The second arrangement consisted only of a 0.030-in.-thick In-metal disk sandwiched between Au foils and irradiated at the same distance from the neutron source as in the first case. The latter packet was covered with 0.01-in.-thick Cd foil. In this second case a similar wrapped packet was positioned at 1 m from the neutron source and 90° from the proton beam line. It was found that room-scattered neutrons produced a negligible effect in the second geometry. The results obtained from counting the In-metal disks and Au foils showed the effects of scattering by the gold, In_2O_3 samples, and Plexiglas capsules. Results were obtained for the 54-min, 4.5-h, and 50-day activation cross sections, and these are listed in Table II in terms of ratios of cross sections in two geometries. The uncertainty estimates in Table II reflect over-all estimates of the precision of these results. These experiments, as well as others, indicated that scattering from the Plexiglas sample holders created most of the observed effect. As the results in Table II bear out, the effects on the (n,n') cross sections are larger than on the (n,γ) cross sections. In the latter case, scattered neutrons are captured by the indium as well as by the gold, whereas in the former case these neutrons are not as likely to cause an (n,n') reaction because of its threshold nature. Within the errors assigned to the scattering corrections, the ratios for the two capture cross sections are the same. This would be expected since the shapes of the cross-section curves are so similar.

TABLE II. Ratios of cross sections obtained in "clean" geometry to cross sections obtained with sample holders in place.

Reaction	Scattering correction at 0.554 MeV	0.813 MeV	1.031 MeV
$In^{113}(n,\gamma)\,In^{114m}$	1.06±0.05	···	1.23±0.12
$In^{115}(n,\gamma)\,In^{116m}$	1.09±0.03	1.15±0.03	1.15±0.03
$In^{115}(n,n')In^{115m}$	1.21±0.04	1.32±0.04	1.30±0.04

Although these scattering experiments, which were done after the primary experiments, indicated that a better choice of sample-holder material might have been made, the corrections were determined well enough that little additional error was introduced into the final values of the cross sections.

Results

Corrections were made where necessary for the effect of the second neutron group from the neutron-source reaction. The results of Buccino *et al.*[25] for the $Li^7(p,n)Be^{7*}$ angular distributions were used. In calculating this correction, the shapes of the In capture-cross-section curves below 0.36 MeV were taken from the work of Cox[26] and Gibbons.[27]

The $Au^{197}(n,\gamma)Au^{198}$ cross sections were taken from the work of Vaughn *et al.*[28] who have considered the data in the literature and have arrived at a curve of cross section versus energy. In the energy region of importance here, this curve is very similar to one at which Gibbons[29] has arrived. It is estimated herein that

[23] Obtained from Oak Ridge National Laboratory.

[24] These are discussed in a general way by R. A. Allen, in *Alpha-, Beta-, and Gamma-Ray Spectroscopy*, edited by K. Siegbahn (North-Holland Publishing Co., Amsterdam, 1965), Vol. I, p. 425.

[25] S. G. Buccino, C. E. Hollandsworth, and P. R. Bevington, Nucl. Phys. **53**, 375 (1964); P. R. Bevington (private communication).

[26] S. A. Cox, Phys. Rev. **133**, B378 (1964).

[27] J. H. Gibbons, R. L. Macklin, P. D. Miller, and J. H. Neiler, Phys. Rev. **122**, 182 (1961).

[28] F. J. Vaughn, K. L. Coop, H. A. Grench, and H. O. Menlove, Bull. Am. Phys. Soc. **11**, 753 (1966).

[29] J. H. Gibbons (private communication). Details available from Sigma Center, Brookhaven National Laboratory.

TABLE III. Estimates of uncertainty in the absolute values of the activation cross sections for the long-lived activities.

Source of uncertainty	Percent error (S.D.) $In^{113}(n,n')In^{113m}$	$In^{113}(n,\gamma)In^{114m}$	$In^{115}(n,n')In^{115m}$	$In^{115}(n,\gamma)In^{116m}$
Counting statistics and area determinations	±4	±5	±4	±3
Scattering correction	±5	±5	±3	±3
Neutron energy	≤7	<1	≤24	<1
$Au^{197}(n,\gamma)Au^{198}$ cross section	±5	±5	±5	±5
Relative counting efficiency	±2	±4	±3	±5
Decay scheme	±2	±7	±3	±4
Combined uncertainty	±(9–11)	±11[a]	±(8–25)	±9

[a] See text for clarification of this value.

the curve used has an accuracy of ±5% in absolute value in the energy range considered here.

The average neutron energies and Au cross sections were obtained with a computer code by numerical integration over the Li target thickness and over the angular spread of the sample sandwich, weighting appropriately to take into account the neutron-source-reaction angular distributions[30] and the angular variation of sample thickness seen by the neutrons.

The scattering corrections at the various energies were obtained from smooth curves drawn through the results given in Table II. Since the corrections for the production of In^{114m} were the same within the limits of error as those for In^{116m}, but the uncertainties for the former were larger, the scattering-correction curve for In^{116m} was used for In^{114m}. However, an additional uncertainty of ±2% has been included in the In^{114m} scattering corrections. Likewise, for In^{113m}, where the correction was not directly measured, the results for In^{115m} were used with an additional ±2% uncertainty introduced.

The major known sources of error in the cross sections are summarized in Table III. The uncertainties throughout this paper in discussion of the present work are listed in terms of standard deviations (S.D.). The estimated percent error from each effect as well as the over-all uncertainty obtained by quadratures are listed. The error in cross section due to a ±3-keV uncertainty in average neutron energy has been included. This estimate of error in energy arises from uncertainties in geometry, energy calibration, and Li target thickness. This contribution is only important for the (n,n') cross sections near threshold; for example, it contributes a ±24% error in the value of the $In^{115}(n,n')In^{115m}$ cross section at 0.361 MeV. For such steeply rising cross sections, the neutron-energy assignment is very important. Smooth curves were drawn through the six sets of cross-section results. Average cross sections at each energy point were obtained from these curves in the same way as they had been obtained from the $Au^{197}(n,\gamma)Au^{198}$ cross-section curve. The cross sections from the curves at the average neutron energies were also obtained. The energy assignment for a given cross-section value was considered good when the average cross section derived from the curve was the same as the cross section from the curve at the average neutron energy. Except for the 0.361-MeV point for $In^{115}(n,n')In^{115m}$, these values were the same within 2%. In that one case, the energy has been lowered by 2 keV from the value given by the computer code to compensate for the difference found. The over-all error for the $In^{113}(n,\gamma)In^{114m}$ cross section is 2% less than that obtained from combining the errors in Table III. This occurs because, as mentioned earlier, an alternate method for obtaining the reaction yield was also used and gave good agreement with the primary method. The uncertainties in the alternate method were ±6% in absolute crystal efficiency for counting the 412-keV γ ray of Au^{198} and ±5% in the In^{114m} disintegration-rate measurement.

The cross-section results are given in Table IV and Figs. 5–13. Also listed in the table are the average neutron energy, the average $Au^{197}(n,\gamma)Au^{198}$ cross section relative to which the In results were obtained, and $\frac{1}{2}$ the full neutron-energy spread from both geometrical and target-thickness effects. If more accurate information on the $Au^{197}(n,\gamma)Au^{198}$ cross sections or decay schemes should become available, the results in Table IV may be renormalized.

Short-Lived Activities

Experiments

The irradiation geometry used in determining the $In^{113}(n,\gamma)In^{114g}$ and $In^{115}(n,\gamma)In^{116g}$ activation cross sections was similar to that used for production of the long-lived activities. A pneumatic tube was used to transfer the $In^{115}{}_2O_3$ sample to the counting apparatus for the 14-sec activations, whereas the $In^{113}{}_2O_3$ was transferred by hand for the 72-sec activations.

Two or more irradiations were needed at each energy to produce sufficient counts. A leaky-capacitor neutron-number integrator was devised for use with these short irradiations. Its principle of operation was similar to that of a leaky-capacitor current integrator.[31] Its use helped ensure that at a given energy the activity

[30] S. J. Austin (private communication).

[31] S. C. Snowdon, Phys. Rev. 78, 299 (1950).

TABLE IV. Cross-section results for production of the long-lived activities.

E_n[a] (MeV)	ΔE_n[b] (MeV)	σ_{Au}[c] (mb)	Cross section (mb) $In^{113}(n,n')In^{113m}$	$In^{113}(n,\gamma)In^{114m}$	$In^{115}(n,n')In^{115m}$	$In^{115}(n,\gamma)In^{116m}$
0.361	0.027	212.3	...	279±31[d]	0.0678±0.0169[d]	184±17[d]
0.448	0.032	174.5	1.01±0.11[d]	225±25	1.51 ±0.13	174±16
0.519	0.032	151.2	2.35±0.22	184±20	2.71 ±0.22	171±15
0.599	0.041	132.1	4.10±0.37	229±25	5.23 ±0.47	188±17
0.662	0.036	120.4	7.21±0.70	236±26	11.8 ±1.0	194±17
0.715	0.034	112.5	12.2 ±1.1	229±25	14.5 ±1.2	188±17
0.772	0.037	106.2	23.0 ±2.1	248±27	22.5 ±1.8	202±18
0.834	0.037	101.1	31.4 ±2.8	263±29	30.5 ±2.4	198±18
0.895	0.035	97.0	37.4 ±3.4	250±28	45.7 ±3.7	209±19
0.958	0.031	93.5	43.1 ±3.9	256±28	56.1 ±4.5	197±18
1.017	0.032	90.8	47.1 ±4.2	280±31	65.6 ±5.2	199±18

[a] Neutron energy in laboratory system.
[b] One-half the full neutron-energy spread.
[c] The $Au^{197}(n,\gamma)Au^{198}$ cross-section values relative to which the In cross sections are given.
[d] Uncertainty (S.D.) in absolute value of the cross section.

produced at the end of each irradiation was the same. Since the Li targets were not perfectly uniform, leaky-capacitor neutron-number integration was, in principle, better than leaky-capacitor current integration. Square-wave pulses from the gate output of a single-channel pulse-height analyzer on the amplifier connected to the neutron monitor were fed into a ratemeter circuit. The time constant of the circuit was adjusted with a uniform input rate from a pulser to correspond to 14 or 72 sec as appropriate. The direct-current output of the circuit was monitored, and the irradiation was automatically terminated when a specified voltage level was reached. As a check on this method, the cross-section calculations were also performed assuming a constant neutron flux over the measured irradiation time.

The samples were counted in close geometry on a 2-in.-diam×1.5-in. plastic scintillator in order to detect the β-ray activity. Amplified pulses were fed into a 400-channel pulse-height analyzer which was operated in the dwell mode at 1 sec per channel. The upper- and lower-level discriminators on the analyzer were adjusted to optimize the ratio of the counts from the activity investigated to counts from background and from other activities.

At each energy, the data summed from two or more irradiations were separated into half-life components using a least-squares computer program. The fits to the data were good.

The β-counting efficiencies necessary for calculating fast-neutron cross sections were determined by making thermal-neutron bombardments. Since cross sections for formation of both In^{114g} (72 sec) and In^{116g} (14 sec), as well as the Au activation cross section, are all known for thermal neutrons, it is possible to solve the appropriate cross-section expression for the desired β-counting efficiency. Thermal neutrons were produced by surrounding the samples with 5 in. of paraffin between the neutron source and sample and at least 8 in. of paraffin on all other sides. Cadmium-ratio measurements were made to determine the effects of nonthermal neutrons; these effects were taken into account in the cross-section calculations. The percentage of activity produced by epi-cadmium neutrons was about 2% for Au^{198} and In^{116g}, and 14% for In^{114g}. Irradiations were also made with less moderator in order to check the validity of the procedure for subtracting the activity due to epi-cadmium neutrons. Supplementary thermal irradiations were also made to determine the effects of neutron absorption in the samples, and the corresponding corrections were applied to the data where necessary.

In other experiments at a neutron energy of about 0.72 MeV, it was found that neutrons scattered from the room and from the apparatus which held the sample sandwich in position produced a negligible effect on the calculated cross sections.

TABLE V. Estimates of uncertainty in the absolute values of the activation cross sections for the short-lived activities.

Source of uncertainty	Percent error (S.D.) $In^{113}(n,\gamma)In^{114g}$	$In^{115}(n,\gamma)In^{116g}$
Counting statistics and reproducibility	± 3	± 5
Scattering correction	± 5	± 5
$Au^{197}(n,\gamma)Au^{198}$ cross section	± 5	± 5
Thermal cross section	±33	±10
Counting efficiency	± 5	± 7
Combined uncertainty	±34	±15

Results

The thermal activation cross sections[7,32] that were used in calculating the β-counting efficiencies were 3±1 b for $In^{113}(n,\gamma)In^{114g}$, 42±4 b for $In^{115}(n,\gamma)In^{116g}$, and 98.8±0.3 b for $Au^{197}(n,\gamma)Au^{198}$.

Corrections were made where necessary for the second neutron group from the $Li^7(p,n)Be^7$ reaction. Table V summarizes the sources of uncertainty in the fast-neutron cross sections. Because of leaky-capacitor-neutron-integrator instabilities, the $In^{115}(n,\gamma)In^{116g}$ cross sections fluctuate somewhat more than counting

[32] *Brookhaven National Laboratory Report No. BNL-325* (U.S. Government Printing Office, Washington, D. C., 1958), 2nd ed.

statistics would account for. An error of ±5%, based upon the scatter of the final values about a smooth curve, is estimated for these fluctuations. In the case of the $In^{113}(n,\gamma)In^{114g}$ cross section, counting statistics account for the observed fluctuations. The uncertainties introduced in the corrections for neutron absorption in the samples and for lack of complete neutron thermalization lead to the assigned errors of β-counting efficiency.

The corrections for scattering in the samples and holders were taken from the results discussed above for the $In^{115}(n,\gamma)In^{116m}$ reaction. Since the shapes of the cross-section curves are very similar for all of the In capture cross sections, this procedure seems valid. The uncertainties in the scattering corrections were the same as those assigned to the 50-day activations.

The final cross-section values are given in Tables VI and VII. For $In^{113}(n,\gamma)In^{114g}$, three irradiations were performed at 0.614 MeV and the maximum spread in the results was about 5%. For $In^{115}(n,\gamma)In^{116g}$, two irradiations were carried out at 0.522 MeV and the results differed by about 7%; three bombardments were made at 0.719 MeV and the maximum spread in the results was about 2%.

Values and uncertainties were also calculated for the total capture cross sections ($\sigma_m+\sigma_g$) of In^{113} and of In^{115}, the composite cross section for $In(n,\gamma)$, and the isomer ratios $\sigma_m/(\sigma_m+\sigma_g)$. In order to obtain the uncertainties in these quantities, the uncorrelated errors in the components, such as those arising from counting statistics, were first suitably combined. The resultant uncertainties were then appropriately combined with the errors common to measurements of the various cross sections (e.g., the uncertainty in the Au cross section). This latter step was, of course, not performed for the isomer-ratio errors.

TABLE VI. The $In^{113}(n,\gamma)In^{114g}$ activation-cross-section results.

E_n[a] (MeV)	ΔE_n[b] (MeV)	σ_{Au}[c] (mb)	$In^{113}(n,\gamma)In^{114g}$ cross section (mb)
0.368	0.029	209.8	68.5±23.3[d]
0.453	0.028	172.4	60.7±20.6
0.530	0.026	148.3	63.0±21.4
0.614	0.028	128.6	68.0±23.1
0.674	0.027	118.3	66.2±22.5
0.723	0.027	111.5	68.1±23.2
0.784	0.027	105.0	68.1±23.2
0.850	0.027	99.9	69.6±23.7
0.908	0.030	96.2	70.0±23.8
0.965	0.030	93.2	70.7±24.0
1.022	0.030	90.5	70.5±24.0

[a] Neutron energy in laboratory system.
[b] One-half the full neutron-energy spread.
[c] The $Au^{197}(n,\gamma)Au^{198}$ cross-section value relative to which the $In^{113}(n,\gamma)In^{114g}$ cross section is given.
[d] Uncertainty (S.D.) in absolute value of the cross section.

TABLE VII. The $In^{115}(n,\gamma)In^{116g}$ activation-cross-section results.

E_n[a] (MeV)	ΔE_n[b] (MeV)	σ_{Au}[c] (mb)	$In^{115}(n,\gamma)In^{116g}$ cross section (mb)
0.365	0.026	211.8	54.7±8.2[d]
0.449	0.028	173.9	66.1±9.9
0.522	0.030	150.5	56.8±8.5
0.611	0.027	129.3	62.9±9.4
0.666	0.027	119.7	59.9±9.0
0.719	0.028	112.1	61.5±9.2
0.773	0.032	106.1	60.6±9.1
0.844	0.028	100.3	61.7±9.3
0.904	0.028	96.5	54.6±8.2
0.959	0.030	93.5	61.4±9.2
1.019	0.029	90.7	48.6±7.3

[a] Neutron energy in laboratory system.
[b] One-half the full neutron-energy spread.
[c] The $Au^{197}(n,\gamma)Au^{198}$ cross-section value relative to which the $In^{115}(n,\gamma)In^{116g}$ cross section is given.
[d] Uncertainty (S.D.) in absolute value of the cross section.

Comparisons with Other Experimental Results

In the energy range covered by the present experiments no other results have been published for the $In^{113}(n,\gamma)In^{114m,114g}$ and $In^{113}(n,n')In^{113m}$ activation cross sections. The present results for $In^{113}(n,\gamma)In^{114m,114g}$ are shown in Fig. 5; those for $In^{113}(n,n')In^{113m}$ are indicated in Figs. 9 and 10.

Aside from other work done in this laboratory,[33,34] the $In^{115}(n,\gamma)In^{116m}$ cross section has been studied the most recently by Cox[26] and by Johnsrud *et al.*[35] Their results

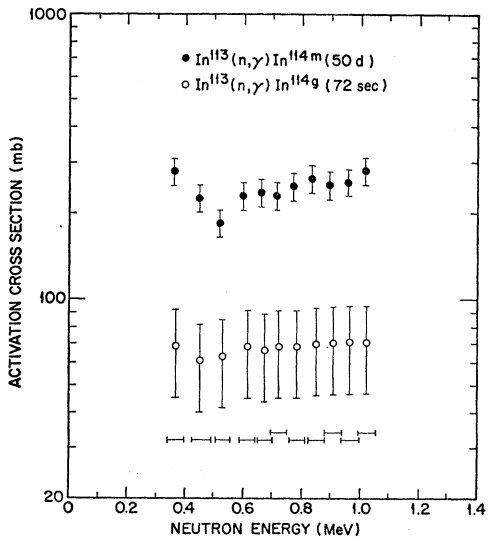

FIG. 5. The $In^{113}(n,\gamma)In^{114m,114g}$ activation-cross-section results. Uncertainties in absolute values of the cross sections are indicated. Full neutron-energy spreads for the $In^{113}(n,\gamma)In^{114g}$ results are shown.

[33] H. O. Menlove, K. L. Coop, H. A. Grench, and R. Sher, U. S. Atomic Energy Commission Report No. CONF-660303, 1966, Book 2, p. 746 (unpublished); Bull. Am. Phys. Soc. **11**, 655 (1966).
[34] H. O. Menlove, K. L. Coop, and H. A. Grench, Lockheed Palo Alto Research Laboratory Report No. LMSC-6-76-66-18, 1966 (unpublished).
[35] A. E. Johnsrud, M. G. Silbert, and H. H. Barschall, Phys. Rev. **116**, 927 (1959).

were obtained relative to values for the $U^{235}(n,f)$ fast-neutron cross section taken from the curve of Allen and Henkel.[36] Counting efficiencies were obtained from the results of thermal irradiations, relying on published thermal-cross-section values. The $Au^{197}(n,\gamma)Au^{198}$ cross-section curve which was used in the present work was obtained after renormalizing those results which were obtained relative to the $U^{235}(n,f)$ cross section to values from a more recent curve[37] for the fission cross section. Therefore, in order to be consistent with this procedure, the results of Cox and of Johnsrud *et al.* were renormalized to values from this same fission-cross-section curve. In the energy range of the present results, this renormalization was always less than 3%. Both sets of results were also renormalized in accordance with recent recommended values of 577.1±0.9 b for the U^{235} thermal fission cross section[37] and 157±4 b for the $In^{115}(n,\gamma)In^{116m}$ thermal activation cross section.[7] A comparison of the present results with these renormalized values of Cox and Johnsrud *et al.* is indicated in Fig. 6. The agreement in the normalization between the present results and the two other sets is good; however, some differences in the shapes of smooth curves drawn through the sets of results may possibly be indicated.

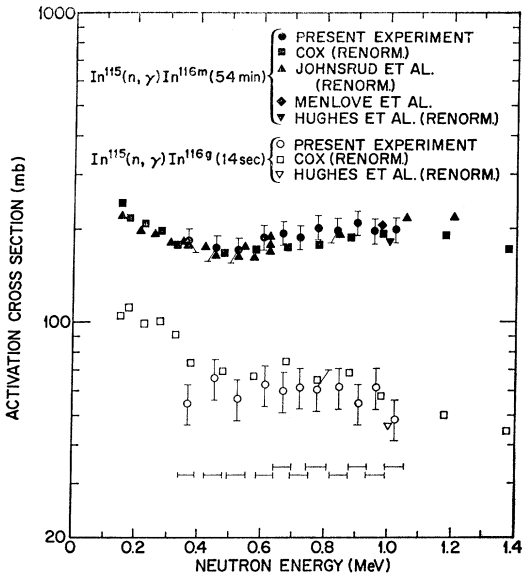

FIG. 6. The present $In^{115}(n,\gamma)In^{116m,116g}$ activation-cross-section results compared with those of Cox (Ref. 26), Johnsrud *et al.* (Ref. 35), and Hughes *et al.* (Refs. 38 and 39), where those latter results have been renormalized as discussed in the text. Also shown is a result of Menlove *et al.* (Refs. 33 and 34). For the present results, uncertainties in the absolute-cross-section values are shown. Full neutron-energy spreads for the $In^{115}(n,\gamma)In^{116g}$ reaction are also indicated.

Hughes *et al.*[38,39] measured the $In^{115}(n,\gamma)In^{116m}$ cross section using a fission spectrum of neutrons whose effective energy was taken as 1 MeV. This measurement has been renormalized to the 157-b value for the thermal cross section, and the result is also plotted in Fig. 6. The renormalized value lies about 10% below the present results; this measure of agreement seems quite satisfactory. The result of Menlove *et al.*,[33,34] obtained relative to the $U^{235}(n,f)$ cross section, is in very good agreement with the present results. Results of earlier work on the $In^{115}(n,\gamma)In^{116m}$ cross section have been summarized by Hughes *et al.*[38] and are also contained in Ref. 32.

The present results for the $In^{115}(n,\gamma)In^{116g}$ activation cross section are also shown in Fig. 6. The results of Cox[26] are shown for comparison; they have been renormalized to the later values of the fission cross section mentioned earlier and the 42-b thermal activation cross section used in the present work. Again, the agreement between the present results and those of Cox is quite satisfactory. The results of Hughes *et al.*[38,39] for this cross section, renormalized to the above value for the thermal cross section, are indicated in Fig. 6. The only other published work on this cross section was performed by Henkel and Barschall.[40] When their result at 1 MeV is renormalized to newer $B(n,\alpha)$ cross-section results, as suggested by Johnsrud *et al.*,[35] and to the 42-b thermal cross section, the resulting value is considerably below the other results and is not shown in Fig. 6.

The fast-neutron capture cross section of indium has been measured, using capture-tank techniques, by Diven *et al.*[41] and by Gibbons *et al.*[27] The present results for the four capture (activation) cross sections can be suitably combined in order to obtain values which can be compared with these $In(n,\gamma)$ capture-tank results. The comparisons are shown in Fig. 7. The uncertainties in the absolute values of the present $In(n,\gamma)$ composite results are about ±8%. The values of Diven *et al.* have been renormalized to more recent values[37] of the U^{235} capture-plus-fission cross section; the results have a normalization uncertainty of ±11% and relative errors of about ±7%. Since the results of Diven *et al.* are about 17% higher than those reported here, the sets of results agree within the error-bar overlap. The results of Gibbons *et al.*, which have ±(11–15)% uncertainties between 0.2 and 0.4 MeV, are about 25% lower than the present values. This discrepancy is somewhat outside the limits given by the combined quoted errors. Bogart[42] has attempted to explain systematic dis-

[36] W. D. Allen and R. L. Henkel, in *Progress in Nuclear Energy*, edited by D. J. Hughes, J. E. Sanders, and J. Horowitz (Pergamon Press, Inc., New York, 1958), Ser. I, Vol. II, p. 1.

[37] *Brookhaven National Laboratory Report No. BNL-325* (U. S. Government Printing Office, Washington, D. C., 1965), 2nd ed., Suppl. 2, Vol. III.

[38] D. J. Hughes, W. D. B. Spatz, and N. Goldstein, Phys. Rev. **75**, 1781 (1949).

[39] D. J. Hughes, R. C. Garth, and J. S. Levin, Phys. Rev. **91**, 1423 (1953).

[40] R. L. Henkel and H. H. Barschall, Phys. Rev. **80**, 145 (1950).

[41] B. C. Diven, J. Terrell, and A. Hemmendinger, Phys. Rev. **120**, 556 (1960).

[42] D. Bogart, U. S. Atomic Energy Commission Report No. CONF-660303, 1966, Book 1, p. 486 (unpublished).

crepancies between the measurements of Gibbons *et al.* for various capture cross sections and the measurements of other workers.

Results for the $In^{115}(n,n')In^{115m}$ activation cross section are shown in Fig. 8. The results of Martin *et al.*[43] have been lowered by 5% to take into account later decay-scheme information. Their results are considerably higher than the present ones at lower energies, but above about 900 keV there is good agreement. They obtained an absolute normalization at 1.28 MeV for their relative cross-section results. This fact indicates that the discrepancy between the sets of results is primarily one involving the shape of the cross section versus energy rather than a normalization factor. Also shown in Fig. 8 are the results of Ebel and Goodman.[44] Their results were normalized to those of Martin *et al.* at 0.88 MeV. These latter results were the

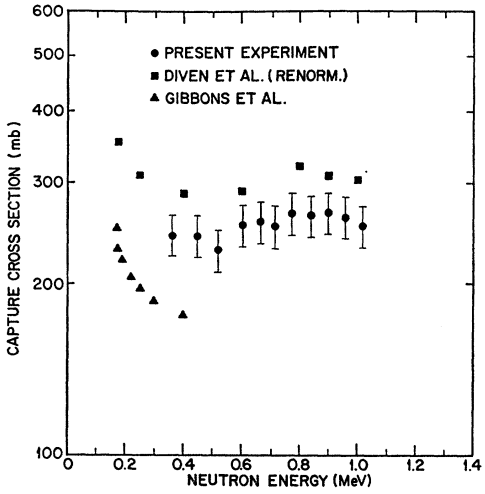

FIG. 7. Composite results of present activation-cross-section measurements compared with the $In(n,\gamma)$ results of Diven *et al.* (Ref. 41), renormalized as discussed in the text, and of Gibbons *et al.* (Ref. 27). For the present results, uncertainties in the absolute-cross-section values are shown.

only values available to Ebel and Goodman at that time in the energy range of interest to them. Although the results of Ebel and Goodman could have been lowered by 5% for consistency, no renormalization has been made since their over-all normalization was arbitrary and since their results are in good agreement with those of the present work, although their points exhibit much more scatter. Vonach and Smith[45] have obtained inelastic-neutron-scattering cross sections for several neutron groups from indium. Although, for neutron energies near threshold, their method does not yield nearly as precise results as the activation method, their results for the sum of the first two inelastic groups are

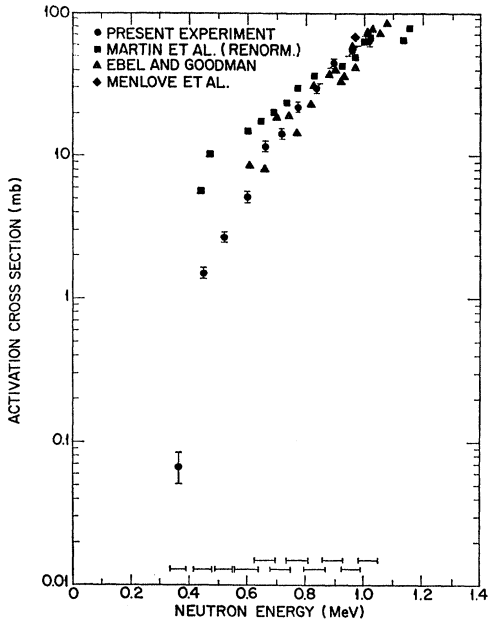

FIG. 8. Comparison of present results for the $In^{115}(n,n')In^{115m}$ activation cross section with those of Martin *et al.* (Ref. 43), renormalized as described in the text, and those of Ebel and Goodman (Ref. 44). Also shown is the result of Menlove *et al.* (Ref. 34). Full neutron-energy spreads and uncertainties in the absolute-cross-section values are shown for the present results.

in agreement with the present work within the assigned limits of error. The result of Menlove *et al.*,[34] indicated in Fig. 8, is in agreement with the present work.

THEORETICAL INTERPRETATION

Introduction

As mentioned earlier, there were two main purposes for the present In cross-section measurements. The first was to ascertain whether calculations using the statistical theory of nuclear reactions and a self-consistent set of the appropriate parameters could fit the six sets of inelastic-scattering and capture results. The parameters would be fixed as much as possible from the results of other types of experiments. Secondly, it was hoped that a comparison of the $In^{113}(n,n')In^{113m}$ activation-cross-section results with the theoretical calculations would make possible a determination of the spin of the second excited state in In^{113}.

The statistical-model formulation used was devised by Hauser and Feshbach[46] for neutron inelastic scattering. Margolis[47] and Lane and Lynn[48] later extended the formulation to neutron capture. An important refinement[48] to the Hauser-Feshbach theory has been the inclusion of the neutron-width-fluctuation correction. Much of the recent theoretical work has been done by

[43] H. C. Martin, B. C. Diven, and R. F. Taschek, Phys. Rev. **93**, 199 (1954).
[44] A. A. Ebel and C. Goodman, Phys. Rev. **93**, 197 (1954).
[45] W. G. Vonach and A. B. Smith, Nucl. Phys. **78**, 389 (1966).
[46] W. Hauser and H. Feshbach, Phys. Rev. **87**, 366 (1952).
[47] B. Margolis, Phys. Rev. **88**, 327 (1952).
[48] A. M. Lane and J. E. Lynn, Proc. Phys. Soc. (London) **A70**, 557 (1957).

Moldauer,[49] who has developed average-cross-section formulas using R-matrix theory. These reduce to the Hauser-Feshbach formulas at certain limits.

The expression used in the present work for the neutron inelastic-scattering cross section is

$$\sigma_{\text{in}}(E,E')=\frac{1}{2(2I+1)}\frac{\pi}{k^2}\sum_{l=0}^{\infty}\sum_{j=|l-1/2|}^{l+1/2}T_n(lj,E)$$

$$\times\sum_{J=|j-I|}^{j+I}\left\{\frac{(2J+1)\sum_{l'j'}[T_n(l'j',E')\mathfrak{R}]}{T_{\text{rad}}(J,E)+\sum_{E''l''j''}T_n(l''j'',E'')}\right\}. \quad (1)$$

In this equation, E is the center-of-mass energy of the incident neutron, k the corresponding wave number, E' the center-of-mass energy of the inelastically scattered neutron, I the target ground-state spin, and l the orbital angular momentum of the incoming neutron. The neutron transmission coefficients $T_n(lj,E)$ were derived from an optical model with spin-orbit coupling and depend, therefore, on whether the neutron spin vector is parallel ($j=l+\frac{1}{2}$) or antiparallel ($j=|l-\frac{1}{2}|$) to the orbital angular-momentum vector. The sum of neutron transmission coefficients in the denominator refers to all permissible outgoing neutron channels from the compound states having spin J and having parity which is determined by the target-nucleus ground-state parity and by the l value. The corresponding sum in the numerator refers only to those permissible channels with energy E'. The pseudo transmission coefficients $T_{\text{rad}}(J,E)$ take into account the competition of γ-ray emission from the original compound-nucleus levels. Finally, the neutron-width-fluctuation corrections $\mathfrak{R}$ depend upon the particular ingoing and outgoing channels.

Details of the calculation of $T_{\text{rad}}(J,E)$ have been given previously[21,50]; the reader is referred to those papers for a description of the parameters used in calculating these quantities. The expression for neutron capture, which is analogous to Eq. (1), is also given there. The fast-neutron-capture isomer-ratio theory used in connection with the present experiment has also been described previously.[6,50,51]

Theoretical Calculations

Figure 9 shows a comparison of experimental results for the $In^{113}(n,n')In^{113m}$ activation cross section with theoretical predictions. Above 0.65 MeV, where inelastic scattering to the 0.65-MeV state leads to increased activation of In^{113m}, predictions using each of the three possible spin assignments for this state are shown. Transmission coefficients were calculated using the ABACUS code[52] and the optical-model parameters

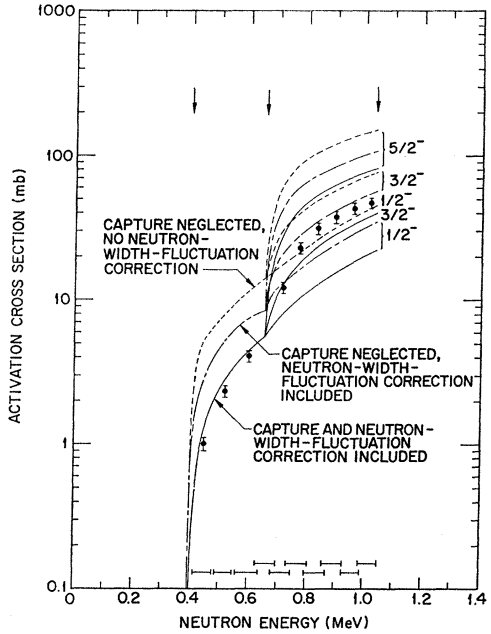

FIG. 9. The $In^{113}(n,n')In^{113m}$ activation cross sections compared with results of the theoretical calculations discussed in the text. The neutron transmission coefficients of Moldauer ($c=0.5$ F) were used. Curves for three spin choices for the 0.648-MeV level are shown. The thresholds for excitation of the excited states are marked. Full neutron-energy spreads and uncertainties in absolute values of the cross sections are also indicated.

of Moldauer [see Eq. (8) of Ref. 53 for the parameters used]. As indicated on the figure, three sets of theoretical results are shown. The first are the results of calculations using the earliest version of the theory,[46] in which both competition from neutron capture and the effects of neutron-width fluctuations are neglected [$T_{\text{rad}}(J,E)=0$ and $\mathfrak{R}=1$]. The fit to the data below 0.65 MeV is so poor that it is clearly not possible to make a valid spin choice based on comparison between experimental and theoretical results above 0.65 MeV. The effect of including the neutron-width-fluctuation correction, but still neglecting capture, is also shown in Fig. 9. It can be seen that this correction is important near threshold and partially removes the discrepancy below 0.65 MeV. Finally, the effect of also including the proper amount (see below) of neutron capture is indicated in Fig. 9. The agreement below 0.65 MeV is good in this case. Above this energy the $\frac{3}{2}^-$ curve is closest to the experimental results, although agreement between the $\frac{5}{2}^-$ curve and experiment is almost as good. Since there is a tendency below 0.65 MeV for the theoretical predictions to fall relative to the experimental results with increasing energy, the $\frac{3}{2}^-$ curve above 0.65 MeV might be expected to be somewhat low, as is observed. In summary, Fig. 9 illustrates the importance of including neutron-width-fluctuation effects and competition from neutron capture in the

[49] P. A. Moldauer, Rev. Mod. Phys. **36**, 1079 (1964).
[50] H. A. Grench, K. L. Coop, H. O. Menlove, and F. J. Vaughn, Nucl. Phys. **A94**, 157 (1967).
[51] H. A. Grench, K. L. Coop, H. O. Menlove, and F. J. Vaughn, Phys. Letters **20**, 407 (1966).
[52] E. H. Auerbach (private communication).
[53] P. A. Moldauer, Nucl. Phys. **47**, 65 (1963).

theoretical calculations. At 0.5 MeV, for example, the fully corrected curve is about $\frac{1}{3}$ as high as the curve without corrections. The over-all fit of the fully corrected curve appears to be good enough to indicate that $\frac{3}{2}^-$ is the correct choice for the 0.648-MeV state.

Another set of optical-model transmission coefficients which are often used in theoretical calculations are those of Campbell *et al.*[54] When these coefficients are used, the results are somewhat different from those given in Fig. 9. Figure 10 compares the fully corrected results of Fig. 9 with those using transmission coefficients of Campbell *et al.* The $\frac{3}{2}^-$ spin choice still appears to be the best.

The optical-model parameter c in Fig. 10 refers to the distance beyond the nuclear radius that the surface-absorption part of the optical potential is centered. The value $c=0.5$ F [Eq. (8) of Ref. 53] was obtained by Moldauer from the best over-all fit to many data. When $c=0.25$ F is used, which is a better choice for the $In^{115}(n,n')In^{115m}$ fitting (see explanation below and Fig. 12), the agreement below 0.65 MeV is worse for In^{113}.

Moldauer[49] has shown from R-matrix theory that, in general, the optical-model transmission coefficients T_n in Eq. (1) should be replaced by quantities $\langle\theta_{\mu n}\rangle$. In the absence of direct reactions,

$$\langle\theta_{\mu n}\rangle = T_n + (1/Q_n)[1-(1-Q_nT_n)^{1/2}]^2.$$

The quantities Q_n depend upon the details of the statistical properties of the level spacings, partial widths, and total widths. The parameters Q_n are usually expected[49] to be between 0 and 1. The case where all $Q_n=0$ ($\langle\theta_{\mu n}\rangle=T_n$) has already been illustrated in Figs. 9 and 10. Calculations were also made which showed that when all the $Q_n=1$, the fully corrected values are raised, but by less than 10%. The $In^{113}(n,n')In^{113m}$ cross section is, therefore, quite insensitive to the value of Q_n, and therefore is not a good choice for the investigation of the proper value of that parameter.

Theoretical calculations[21,50] of the total capture cross section ($\sigma_m+\sigma_g$) were also made. The results depend upon the following parameters of the compound nucleus: B, the neutron binding energy; β, the ratio of the average radiation width to average level spacing for s-wave levels at the neutron binding energy; a, the parameter appearing in the energy dependence of the nuclear level density; and σ, the spin cutoff factor. The quantity B is 7.312 and 6.725 MeV for In^{114} and In^{116}, respectively.[55] The values for the spin cutoff factor were derived from the fitting of the isomer-ratio results (see below). The quantity a was taken from Eq. (5.4) of Lang[56] which

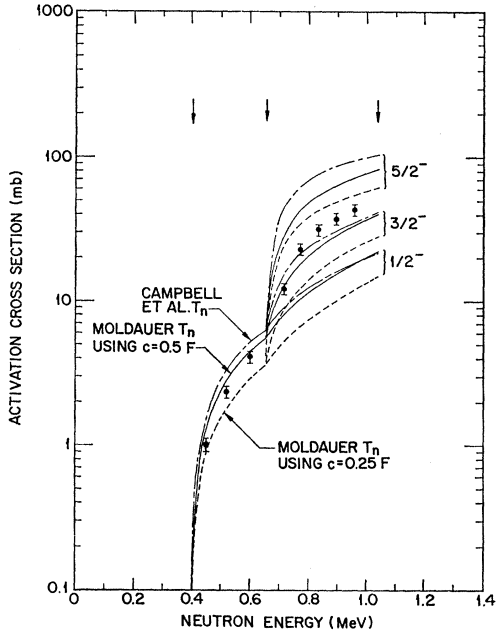

FIG. 10. The $In^{113}(n,n')In^{113m}$ activation cross sections compared with results of the theoretical calculations discussed in the text. The calculations included both competition from neutron capture and the neutron-width-fluctuation correction. Curves for the three spin choices for the 0.648-MeV level are shown. The thresholds for excitation of the excited states are also marked. Uncertainties in absolute-cross-section values are shown.

gives an over-all fit to experimentally derived values for many nuclides; this equation gives $a=17.24$ and 17.44 MeV^{-1} for In^{114} and In^{116}, respectively. However, near mass number 115, values of a between about 10 and 25 MeV^{-1} are allowed within the error limits of the experimental values. The effects of changes in a will be discussed below.

The value of β was chosen which gave a good over-all fit (by eye) to the total capture cross sections. In the case of In^{113}, the calculated total capture cross sections used were those made with the $\frac{3}{2}$ spin choice for the 648-keV level. The values of β were 0.016, 0.0175, and 0.015 when transmission coefficients corresponding to the Moldauer $c=0.5$ F, Moldauer $c=0.25$ F, and Campbell *et al.* optical-model parameters, respectively, were used. The fit to the In^{113} data is shown in Fig. 11 for the Moldauer $c=0.5$ F set of coefficients. The neutron-width-fluctuation correction was included in these calculations and all $Q_n=0$. Between 0.3 and 1.1 MeV the theoretical curves for the other two sets of T_n lie within 6% of the curves shown (for corresponding spin choices). In each case, the value of $\sigma=3.4$ was used. The variation of the ($\sigma_m+\sigma_g$) curves with the spin choice is also illustrated in Fig. 11; the changes are much smaller than for the σ_{in} curves.

The theoretical fast-neutron-capture isomer ratios $[\sigma_m/(\sigma_m+\sigma_g)]$ depend most strongly[6,50,51] upon values for the spin cutoff factor and the average γ-ray multi-

[54] E. J. Campbell, H. Feshbach, C. E. Porter, and V. F. Weisskopf, Massachusetts Institute of Technology Laboratory for Nuclear Science Technical Report No. 73, 1960 (unpublished).

[55] J. H. E. Mattauch, W. Thiele, and A. H. Wapstra, Nucl. Phys. **67**, 32 (1965).

[56] D. W. Lang, Nucl. Phys. **26**, 434 (1961).

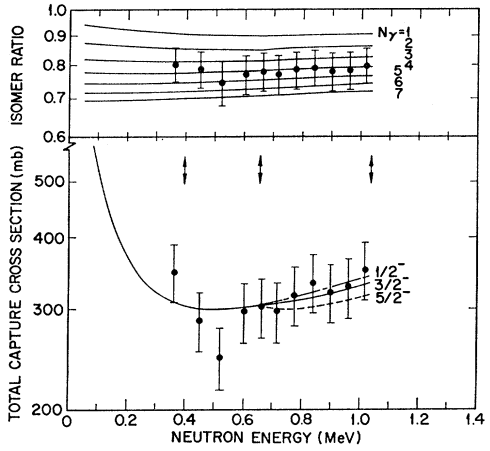

FIG. 11. The In^{113} total capture cross sections and isomer ratios compared with results of the theoretical calculations discussed in the text. For the case of $(\sigma_m+\sigma_g)$, curves corresponding to the possible spin choices for the 0.648-MeV level are shown. For the isomer-ratio curves, the $\frac{3}{2}^-$ choice was used. For all of the curves, the $c=0.5$ F transmission coefficients of Moldauer were used, $\sigma=3.4$, $a=17.24$ MeV^{-1}, and $\beta=0.016$. The thresholds for excitation of the excited states are shown. Uncertainties in absolute values are indicated.

plicity N_γ. Measurements[57–59] of N_γ for the capture of thermal or resonance energy neutrons by indium have yielded values in the range 3.3 to 5.6. Experiments on other target nuclei whose mass is near that of indium have yielded similar values.[57–59] For fast-neutron capture by indium, a value of 4 or 5 seems appropriate.

Theoretical isomer-ratio curves for several values of N_γ are compared with the In^{113} results in Fig. 11 (for the $\frac{3}{2}$ spin choice). The calculations were found to be quite insensitive[50] to the particular set of T_n, a, and β used. The value $\sigma=3.4$ was needed to fit (by eye) the $N_\gamma=4$ calculations to the experimental results; the pair $\sigma=3.7$ and $N_\gamma=5$ produced equally good agreement.

Theoretical calculations of the $In^{115}(n,n')In^{115m}$ activation cross section proceeded as outlined for In^{113}, although more energy levels were involved for In^{115}. The fully corrected results using Moldauer's optical-model parameters with $c=0.5$ F are shown in Fig. 12. Since the fit to the data is much poorer below the threshold for excitation of the second excited state than in the case of In^{113}, the effects of some variations in optical-model parameters were investigated. Vonach and Smith,[45] in fitting their In elastic and inelastic angular-distribution data to theoretical calculations, examined the effects of variations in the imaginary well depth W and the quantity c of the Moldauer parameters. They found that although they could produce somewhat better agreement in specific energy regions for indium, the original set produced satisfactory global fits for silver, indium, and cadmium.

We concentrated on fitting the Vonach and Smith In elastic- and inelastic-scattering angular distributions between 0.3 and 0.8 MeV, the energy region where the In^{115} level assignments were known best. The "best" parameters found from these calculations were $W=13.84$ MeV and $c=0.44$ F. It was found, however, that the choice given by Moldauer, $W=14$ MeV and $c=0.5$ F, produced almost equally good fits. Furthermore, with $W=14$ MeV, values as low as $c=0$ F also produced rather satisfactory results. It therefore seemed reasonable to try transmission coefficients obtained with the parameter choices $c=0$ F and $c=0.25$ F. These were also used in calculations of the $In^{115}(n,n')In^{115m}$ activation cross sections. Results obtained using $c=0$ or 0.25 F gave better fits to the data, at least below the threshold for excitation of the 0.595-MeV state; this is illustrated in Fig. 12. However, as shown earlier, $c=0.25$ F (or 0 F) produces poorer agreement for In^{113}. The lowest-energy point is considerably below the theoretical curve. Moldauer[60] has cautioned, however, that the results of calculations using the average-cross-section formula may not be expected to be in good agreement with experiment at energies close to threshold. This would be expected to be particularly

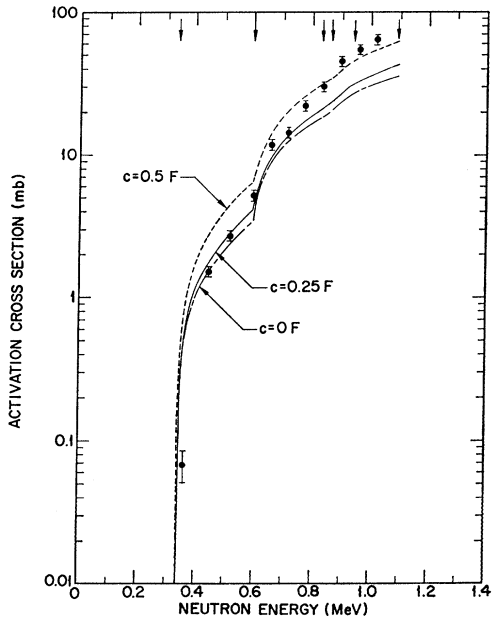

FIG. 12. The present $In^{115}(n,n')In^{115m}$ activation cross sections compared with results of the theoretical calculations discussed in the text. The calculations included both competition from neutron capture and the neutron-width-fluctuation correction. Curves are shown for three sets of transmission coefficients derived from optical-model parameters of Moldauer. The thresholds for excitation of the excited states are marked. Uncertainties in absolute-cross-section values are indicated.

[57] C. O. Muehlhause, Phys. Rev. **79**, 277 (1950).
[58] L. V. Groshev, A. M. Demidov, V. N. Lutsenko, and V. I. Pelekhov, in *Proceedings of the Second United Nations Conference on the Peaceful Uses of Atomic Energy* (United Nations, Geneva, 1958), Vol. 15, p. 138.
[59] J. E. Draper and T. E. Springer, Nucl. Phys. **16**, 27 (1960).
[60] P. A. Moldauer, Phys. Rev. **129**, 754 (1963).

true when the experimental energy spread includes the threshold energy, as it does in the case of this point. It should be mentioned that Vogt *et al.*[61] have done theoretical calculations of the $In^{115}(n,n')In^{115m}$ cross section to extract information concerning the d-wave strength function.

In order to fit the observed In^{115} total capture cross sections, the values $\beta=0.0115$, 0.0125, and 0.0125 were needed for the $c=0.5$ F, 0.25 F, and 0 F coefficients, respectively. The In^{115} isomer ratios were fitted with $\sigma=3.2$ and 3.5 for $N_\gamma=4$ and 5, respectively (see Fig. 13).

The effects on $(\sigma_m+\sigma_g)$ of variations in a are illustrated in Fig. 13 for the $c=0.5$ F coefficients. The values of β have been adjusted to normalize the curves at 0.5 MeV. This normalization resulted in $\beta=0.014$, 0.0115, and 0.01 for $a=10$, 17.44, and 25 MeV^{-1}, respectively. The value $\sigma=3.2$ was the same for the three curves. It is seen that $a=17.44$ MeV^{-1} appears to be a good choice, although the sensitivity to a is not great.

It should be emphasized that the values of β were chosen to fit the present data between 0.36 and 1.02 MeV. Cross sections for $In(n,\gamma)$ predicted using these values would be somewhat higher than the experimental results of Gibbons *et al.*[27] at lower energies. However, since there is some discrepancy between our experimental results and those of Gibbons *et al.* where the sets of measurements overlap, it is not clear to what extent the theoretical predictions are uncertain.

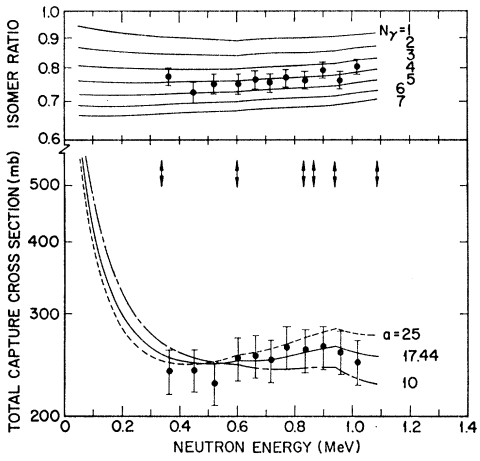

FIG. 13. The present In^{115} total capture cross sections and isomer ratios compared with results of the theoretical calculations discussed in the text. For the $(\sigma_m+\sigma_g)$ curves, values of β were 0.014, 0.0115, and 0.01 for $a=10$, 17.44, and 25 MeV^{-1}, respectively. For the isomer-ratio curves, $a=17.44$ MeV^{-1}. For all the curves, the Moldauer ($c=0.5$ F) transmission coefficients were used and $\sigma=3.2$. The thresholds for excitation of the excited states are shown. Uncertainties in absolute values are indicated.

[61] E. W. Vogt, Phys. Letters **7**, 61 (1963); W. G. Cross, D. McPherson, and E. W. Vogt, Bull. Am. Phys. Soc. **9**, 166 (1964).

TABLE VIII. Ratios of effective nuclear moments of inertia to rigid-body moments for In^{114} and In^{116} which are implied by the values obtained for the spin cutoff factors.

Compound nucleus	Spin cutoff factor	$\mathcal{I}/\mathcal{I}_R$
In^{114}	3.4	0.60
	3.7	0.71
In^{116}	3.2	0.54
	3.5	0.64

Summary

Comparisons of the present experimental results with theoretical calculations for the $In^{113}(n,n')In^{113m}$ and $In^{115}(n,n')In^{115m}$ activation cross sections indicate that effects of competition from neutron capture and of neutron-width fluctuations should be included in the computations. Secondly, a spin-parity choice of $\frac{3}{2}^-$ for the 648-keV state in In^{113} is indicated. Thirdly, a change in Moldauer's optical-model parameters, such as that found for the quantity c, seems to be needed in going from In^{113} to In^{115}.

The total-capture-cross-section comparisons indicate that $\beta\approx0.016$ and 0.0125 for In^{114} and In^{116}, respectively. Measurements[62] in the resonance region indicate Γ_{rad} to be 80 ± 20 and 77 ± 15 meV for In^{114} and In^{116}, respectively, with an average level spacing of 7 ± 1 eV being observed for each nucleus. When Γ_{rad} and D_{obs} values are combined, values of β of 0.011 ± 0.003 are obtained for each of the nuclei. Considering the uncertainties involved in both the experimental results and the theoretical calculations, the agreement between values of β obtained in the two ways seems satisfactory. The theoretical ratio[6,50] for $\beta(In^{114})/\beta(In^{116})$, based upon the mass and binding-energy dependence, is about 2. This can be compared with the value 1.3 obtained from independently fitting theoretical curves for the total capture cross section to experimental results for In^{113} and In^{115}.

Using $N_\gamma=4$ (or 5), values for σ of 3.4 (or 3.7) and 3.2 (or 3.5) were found necessary for In^{114} and In^{116}, respectively. The spin cutoff factor can be related to an effective nuclear moment of inertia.[6,50] The results for In^{114} and In^{116} (with $a=17.24$ and 17.44 MeV^{-1}, respectively) are given in Table VIII in terms of the ratio of the moment of inertia $\mathcal{I}$ to the rigid-body moment $\mathcal{I}_R$. The shell-model prediction[6,50] is $\mathcal{I}/\mathcal{I}_R\approx1.0$ for each nucleus.

ACKNOWLEDGMENTS

The authors wish to gratefully acknowledge the assistance of K. L. Coop who helped perform the experiments and theoretical calculations, of Dr. F. J. Vaughn who developed the computer code for the average neutron energy and Au cross section, and of Dr. E. H. Auerbach for supplying the ABACUS program.

[62] J. A. Harvey, D. J. Hughes, R. S. Carter, and V. E. Pilcher, Phys. Rev. **99**, 10 (1955).